

# SPATIALLY AND TEMPORALLY VARYING DUST LIFTING THRESHOLDS IN A MARTIAN GCM

**D. P. Mulholland, P. L. Read**, Atmospheric, Oceanic & Planetary Physics, University of Oxford, Clarendon Laboratory, Parks Road, Oxford OX1 3PU, UK ([mulholland@atm.ox.ac.uk](mailto:mulholland@atm.ox.ac.uk)), **S. R. Lewis**, Department of Physics & Astronomy, The Open University, Walton Hall, Milton Keynes MK7 6AA, UK, **F. Forget**, Laboratoire de Météorologie Dynamique, Université Paris 6, BP 99, 75005 Paris, France.

## Introduction:

Atmospheric dust is one of the key constituents of the Martian atmosphere, and variations in dust loading can have a profound effect on the development of the mean circulation [1], and affect ice cloud formation [2] and other aspects of the climate system. While parameterisations for predicting rates of dust emission from the surface are now an important part of Martian general circulation models (MGCMs) [3, 4, 5], the high degree of interannual variability and apparent unpredictability in the occurrence of large Martian dust storms [6] has proved difficult to capture in models thus far.

One important reason for this is a limited knowledge of Martian soil properties, and of the spatial and temporal variability of the surface state (particle surface dust density, particle size distribution). Here we use what information there is to produce a physically-based dust lifting scheme for the UKMGCM (a Mars GCM which couples the UK spectral dynamical core to physics from the LMD model [7]) that rivals, as much as possible, the complexity of current terrestrial dust emission parameterisations. Attention is paid to the ability of the model to reproduce observed timings of dust storm initiation and decay, the spatial pattern of surface dust removal, and interannual variability in global dust opacity.

## MGCM dust lifting parameterisations:

Dust lifting in the UKMGCM was originally implemented by [3], and features two parameterised processes, in common with other Mars GCMs [4, 5]. Convective lifting, by ‘dust devils’, occurs at a rate proportional to an activity parameter [8], dependent on the thermodynamic efficiency of the convective heat engine and the sensible heat flux. A threshold-dependency may additionally be imposed, using a cyclostrophic estimate of the tangential wind speed of the vortex. The proportionality constant, defining the efficiency of the lifting process, is tuned to provide model dust opacities in broad agreement with observations over the period  $L_s=0-180^\circ$ , when lifting by other mechanisms is thought to be infrequent.

Greater focus has been applied to the other model dust lifting mechanism, namely near-surface wind stress, reflecting its importance in the development of regional and global dust storms. We calculate the threshold stress for the initiation of dust lifting using equation (24) of [9], applied to sand-sized particles

of diameter  $\sim 180\mu\text{m}$ . Above threshold, micron-sized vertical dust flux is set proportional to the horizontal saltation flux, estimated using a function based on the numerical model of [10]. This functional dependence is similar to the more commonly-used formula of [11], but saltation flux levels off somewhat with increasing frictional velocities, due to the influence of electrostatic effects on saltation. It thus implies a slightly more explosive lifting process than the previously-used flux function.

GCM mean surface winds do not include sub-gridscale windspeed variation and transient gusts, which are of crucial importance to a strongly threshold-dependent process such as wind stress dust lifting. In addition, a two-threshold situation has recently been theorised to exist on Mars [12, 13], implying that very different frictional velocities are required respectively to initiate and subsequently to sustain saltation.

At present, both these considerations have been subsumed into a reductive scaling factor applied to the calculated threshold friction velocity. The value of this factor, determined by the model’s ability to produce significant dust lifting at the correct locations and time of year, and found to be  $\sim 0.7$  at low model resolution (resulting in a threshold stress of around  $0.019\text{Nm}^{-2}$ ), is physically plausible given the order-of-magnitude difference in impact and fluid thresholds found by [13]. This is, however, likely to be a key source of error in the dust lifting scheme, and would benefit from greater insight into small-scale surface wind variability.

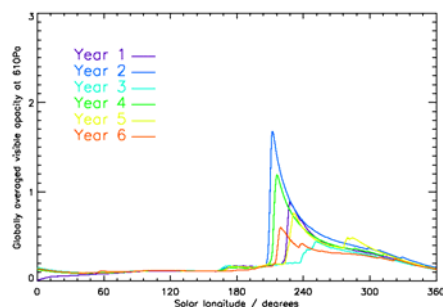


Figure 1: Globally-averaged dust visible opacity from several years of a simulation using unlimited surface dust.

Dust lifting simulations are performed with radiatively-active dust, using several (in this work, either three or six) dust particle size bins, from 0.1-

10 $\mu$ m radius. The size distribution lifted from the surface is fixed, and leads to a seasonal variation in atmospheric effective radii that is in good agreement with observations [14].

#### Dust storm simulation:

Realistic opacities and *some* interannual variability may be produced by the model when assuming an unlimited supply of surface dust (Figure 1); however, very precise tuning of the lifting efficiency and threshold are required. This choice is resolution-dependent, and applying present-day settings to an increased-obliquity model setup (for the simulation of past climates) results in overly vigorous, runaway lifting, suggesting that an incomplete lifting scheme is being used. Furthermore, the extent of the interannual variation in opacity is not as large as is observed. Therefore, an additional component is needed for a realistic lifting parameterization.

#### Surface constraints:

*Variable lifting threshold.* In an attempt to improve the interannual variability in dust opacity produced by the model, as well as making it more robust with respect to lifting parameter values, a surface feedback scheme has been implemented as first suggested by [15] and recently added to a GCM by [16]. The threshold for lifting is allowed to vary in response to the amount of dust removed from or deposited at a particular gridpoint – in this way, the surface state becomes a new dynamic variable, adding a ‘memory’ to the system from one year to the next. Large dust storms are only possible when thresholds at key initiation regions are suitably low.

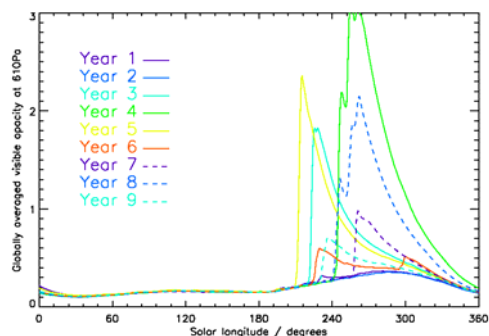


Figure 2: Globally-averaged dust visible opacity from several years of a variable-threshold simulation.

In order to produce realistic multiannual dust opacities, it was necessary to add a (constant) threshold-decrease term, otherwise a steady loss of dust into polar regions and other areas from which it is unlikely to be removed by wind stress lifting leads to an eventual shutdown of dust storms in the model, as lifting thresholds become permanently too high. This decrease, which should be provided by dust deposition, could be accounted for by transport due to dust devil lifting, which is currently excluded from the variable threshold scheme. Work is ongoing to in-

clude both lifting processes in the scheme.

With a suitable threshold decrease rate, multi-year runs which capture a significant portion of the observed variation in dust storm size and timing are possible (Figures 2, 3). Storm initiation occurs over a seasonal window covering  $L_s \sim 210^\circ$ - $300^\circ$ . Large storms typically form whenever a dust front in the northern winter baroclinic region flushes southwards via either the Chryse or Utopia channels, reaches the southern hemisphere and sparks further dust lifting there (similar to, for example, the regional storm which developed at Noachis in MY23 [17]). The peak opacity and size attained by these storms is affected by the southern hemispheric surface state, in particular the thresholds in the Hellas, Noachis and Daedalia Planum regions.

Some amount of wind-stress dust lifting is produced in every year of the simulations, and in each year global opacity returns to its pre-storm value by  $L_s = 0^\circ$ , which is in accordance with the observational record. A realistic range of peak global opacities is obtained during a single simulation. The success of the variable-threshold approach supports the idea that Martian global dust storm development is dependent upon the recent history of dust lifting and transport, and that more than one suitable lifting site is required for a planet-encircling storm to develop.

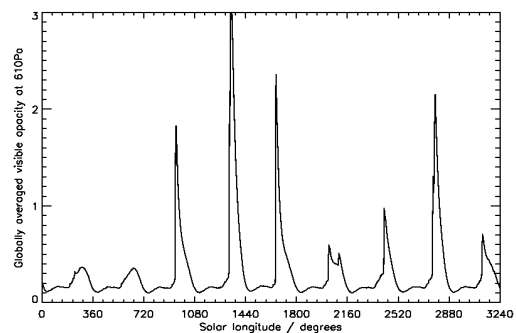


Figure 3: The same output as in Figure 2, but presented chronologically.

Figure 4 shows the change in surface dust density (due to wind-stress lifting) after five model years for one particular simulation. A net loss of dust is seen in southern midlatitudes and along the well-known northern hemisphere storm tracks, while polar regions and the northern hemisphere plains gain dust. This prediction is in good agreement with the ‘dust cover’ map derived by [18], though an underprediction of lifting poleward of  $60^\circ$ S is suggested.

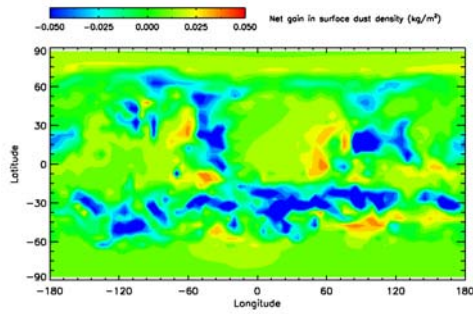


Figure 4: Change in surface dust density after six model years.

*Heterogeneous surface roughness.* Another important consideration in lifting parameterisations is the ‘roughness length’ ( $z_0$ ) of the surface. This parameter controls the strength of the drag on the near-surface wind, and influences the ease with which saltation can eject dust particles from the surface into the atmosphere. In the absence of more information,  $z_0$  has typically been set to a uniform value (1cm in the present case) in MGCMs.

Recently, a global map of  $z_0$  has been calculated from TES data [19, 20] and inserted into the UKMGCM (Figure 5). The most significant changes to the near-surface atmosphere are seen in the northern hemisphere plains, where  $z_0$  values are an order of magnitude or more below the value previously used. In these smooth regions, reduced upward turbulent mixing leads to an increase in surface drag velocities, and a reduction in the near-surface diurnal temperature range of as much as 5K.

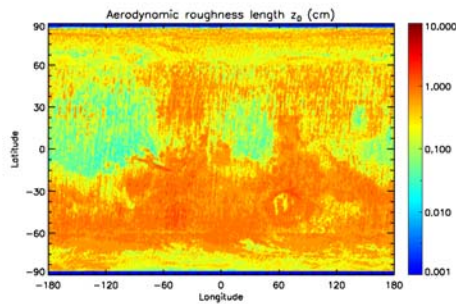


Figure 5: TES-derived surface roughness  $z_0$ .

Rough terrain increases the threshold for wind stress lifting [21], thus the inclusion of the roughness map leads to a rebalancing of the relative ability of various regions of the planet to support dust lifting (note that the source regions from Figure 4 typically correspond to high values of  $z_0$ ). Results will be presented showing the effect of this addition on the modelled dust cycle (used in combination with the variable threshold scheme), including its possible impact on lifting via dust devils.

**References:** [1] Haberle, R. M. et al. (1993), *J. Geophys. Res.*, 98, 3093-3123. [2] Montmessin, F. et al. (2004), *J. Geophys. Res. (Planets)*, 109:100004-+.

[3] Newman, C. E. et al. (2002), *J. Geophys. Res. (Planets)*, 107:5123-+. [4] Basu, S. et al. (2004), *J. Geophys. Res. (Planets)*, 109(E18):11006-+. [5] Kahre, M. A. et al. (2008), *Icarus*, 195:576-597. [6] Zurek, R. W. and Martin, L. J. (1993), *J. Geophys. Res.*, 98, 3221-3246. [7] Forget, F. et al (1999), *J. Geophys. Res.*, 104 24155-24175. [8] Renno, N. O. et al. (2000), *J. Geophys. Res.*, 105:1859-1866. [9] Shao, Y. and Lu, H. (2000), *J. Geophys. Res.*, 105:22437-22444. [10] Kok, J. F. and Renno, N. O. (2008), *Phys. Rev. Lett.*, 100(1):014501-+. [11] White, B. R. (1979), *J. Geophys. Res.*, 84:4643-4651. [12] Claudin, P. and Andreotti, B. (2006), *Earth and Planetary Science Letters*, 252(1-2):30-44. [13] Kok, J. F. (2010), *Geophys. Res. Lett.*, 37, L12202. [14] Wolff, M. J. and Clancy, R. T. (2003), *J. Geophys. Res. (Planets)*. [15] Pankine, A. A. and Ingersoll, A. P. (2002), *Icarus*, 155:299-323. [16] Wilson, R. J. and Kahre, M. A., *Mars Dust Cycle Workshop 2009*. [17] Lewis, S. R. et al. (2007), *Icarus*, 192(2):327-347. [18] Ruff, S. W. and Christensen, P. R. (2002), *J. Geophys. Res. (Planets)*, 107:5127-+. [19] Hebrard, E. et al, *Mars Dust Cycle Workshop 2009*. [20] Forget, F., private communication. [21] Raupach, M. R. et al. (1993), *J. Geophys. Res.*, 98, 3023-3029.